# Oscillatory Active-site Motions Correlate with Kinetic Isotope Effects in Formate Dehydrogenase

Philip Pagano,<sup>1†</sup> Qi Guo,<sup>1†</sup> Chethya Ranasinghe,<sup>1</sup> Evan Schroeder,<sup>1</sup> Kevin Robben,<sup>1</sup> Florian Häse,<sup>2</sup> Hepeng Ye,<sup>1</sup> Kyle Wickersham,<sup>1</sup> Alán Aspuru-Guzik,<sup>2,3</sup> Dan T. Major, <sup>4</sup> Lokesh Gakhar,<sup>5</sup> Amnon Kohen<sup>1</sup> and Christopher M. Cheatum<sup>1\*</sup>

- <sup>1</sup>Department of Chemistry, University of Iowa, Iowa City, IA 52242, United States
- <sup>2</sup>Department of Chemistry and Chemical Biology, Harvard University, Cambridge, MA 02138, United States
- <sup>3</sup> Senior Fellow, Canadian Institute for Advanced Research (CIFAR), Toronto, Ontario M5G 1Z8, Canada
- <sup>4</sup>Chemistry Department, Bar-Ilan University, Ramat Gan 52900, Israel
- <sup>5</sup>Protein Crystallography Facility and Department of Biochemistry, University of Iowa, Iowa City, Iowa 52242, United States
- \*To whom correspondence should be addressed; email: <a href="mailto:christopher-cheatum@uiowa.edu">christopher-cheatum@uiowa.edu</a>

### Abstract

Thermal motions of enzymes have been invoked to explain the temperature dependence of kinetic isotope effects (KIE) in enzyme-catalyzed hydride transfers. Formate dehydrogenase (FDH) from *Candida boidinii* exhibits a temperature independent KIE that becomes temperature dependent upon mutation of hydrophobic residues in the active site. Ternary complexes of FDH that mimic the transition state structure allow investigation of how these mutations influence active-site dynamics. A combination of X-ray crystallography, two-dimensional infrared (2D IR) spectroscopy, and molecular dynamic simulations characterize the structure and dynamics of the active site. FDH exhibits oscillatory frequency fluctuations on the picosecond timescale, and the amplitude of these fluctuations correlates with the temperature dependence of the KIE. Both the kinetic and dynamic phenomena can be reproduced computationally. These results provide experimental evidence for a connection between the temperature dependence of KIEs and motions of the active site in an enzyme-catalyzed reaction consistent with activated tunneling models of the hydride transfer reaction.

**KEYWORDS** Protein dynamics, enzyme catalysis, two-dimensional infrared spectroscopy, KIE, formate dehydrogenase, oscillation, dynamics

<sup>&</sup>lt;sup>†</sup>These two authors contributed equally to this work.

### Introduction

The role of enzyme dynamics in enzyme-catalyzed reactions is of significant interest for rational drug design and molecular-evolutionary studies. <sup>1-12</sup> Enzyme dynamics encompass motions that span a broad range of timescales. The role of motions at the femtosecond (fs) to picosecond (ps) timescales in enzyme-catalyzed bond activation, <sup>2-5, 7, 11, 13-17</sup> is hotly debated, but motions at these timescales are difficult to experimentally characterize and therefore not well understood. Primary kinetic isotope effect (KIE) studies suggest that fast protein motions may play an important role in facilitating enzyme-catalyzed hydride transfer; <sup>18-26</sup> however, those

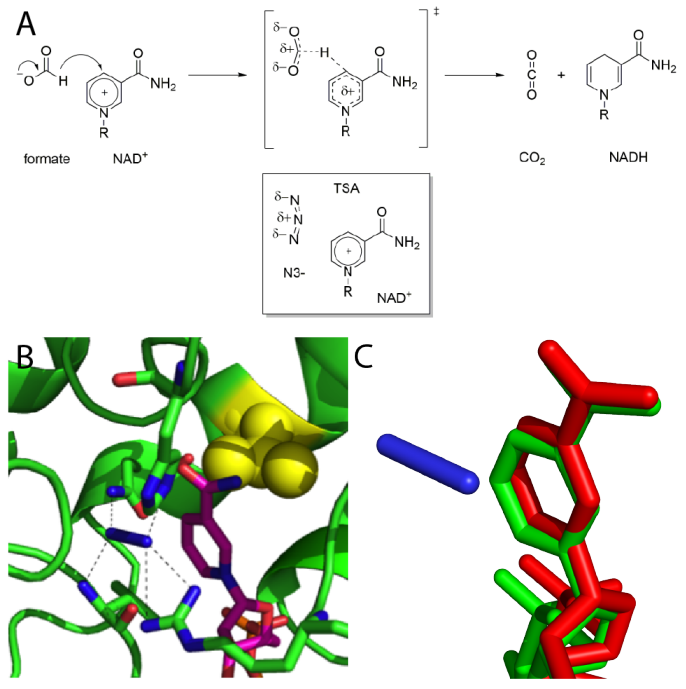


**Figure 1** A) Reaction scheme for the hydride transfer between formate and NAD<sup>+</sup> catalyzed by FDH. The azide anion forms a ternary complex with FDH that mimics the transition state structure. B) The active site of wild-type CbFDH (PDB 5DN9) with the two ligands (azide in blue and NAD<sup>+</sup> in magenta) shows the mutation site, V123, as yellow spheres. C) Crystal structures of WT FDH (Green) and V123A FDH variants (red, PDB 6D4B) reveal displacement of the C4 position of the nicotinamide ring with respect to the central nitrogen of azide, which is analogous to displacement of the DAD in the enzymecatalyzed reaction.

studies fall short of answering this
question directly, since they cannot report
on the timescales on which the active site
or the reacting substrates fluctuate.
Correlating kinetic effects on hydride
transfer with fast dynamics of the enzyme
has been a longstanding goal but requires

a system in which both can be measured.

Formate dehydrogenase (FDH, EC 1.2.1.2, uniport code O13437), offers a convenient opportunity to study active-site dynamics with relevance to the chemical step on the fs–ps timescale. FDH is a homodimer with two independent active sites <sup>27</sup> and catalyzes the irreversible

hydride transfer from formate to the C4 position of the nicotinamide ring of nicotinamide adenine dinucleotide (NAD<sup>+</sup>), giving CO<sub>2</sub> and NADH (Figure 1 A). <sup>28-31</sup> FDH is an attractive system for correlating kinetics and dynamics since it allows investigation of both kinetic isotope effect measurements (KIEs), which can probe the nature of the hydride transfer reaction, <sup>29, 32</sup> and vibrational spectroscopy, which can reveal active site motions, using an excellent structural analog of the activated complex, azide. Azide is both a tight-binding, competitive inhibitor  $(K_i = 7 \text{ nM}^{28} \text{ and } K_D = 40 \text{ nM})$  and a convenient IR chromophore, allowing us to probe motions of the enzyme in a structure analogous to the tunneling ready state (TRS). Wild-type (WT) FDH exhibits temperature-independent intrinsic kinetic isotope effects (KIEs), <sup>29, 32</sup> indicating that the donor-acceptor distance (DAD) at the TRS is narrowly distributed at a short distance, i.e. well organized for H-tunneling.<sup>7,29</sup> In addition, two-dimensional infrared spectroscopy (2D IR), which probes the antisymmetric stretch of the azide anion bound to the FDH-NAD<sup>+</sup>-azide ternary complex, reports the fs-ps motions of the active site. 33-37 Because both the kinetic and dynamic behavior can be directly measured without perturbing the enzyme, FDH is an ideal system for investigating active-site dynamics and how they may influence hydride transfer.

Here we characterize the temperature dependence of KIEs and use 2D IR to investigate active-site dynamics via structurally guided mutagenesis of relevant active-site residues. <sup>22, 38, 39</sup> These experiments address whether or not the temperature dependence of KIEs report on dynamic phenomena related to DAD sampling at timescales relevant to hydride transfer. There are two prevailing models for the role of such dynamics in enzyme-catalyzed hydride transfer reactions: activated tunneling and protein promoting vibrations. Activated tunneling models make an adiabatic separation between the relatively fast motion of the hydrogen nucleus and the slower motions of the environment, in this case the protein. The transition state of the reaction in

this model is characterized by degeneracy in the double-well potential for the hydrogen motion between the hydride donor and acceptor. Because the motions of the environment to approach this state involve reorganization of degrees of freedom other than the hydrogen motion, these contributions to the rate are isotopically insensitive and do not contribute to the observed KIE. The KIE, is then dominated by the probability of hydrogen transfer between the two wells of the double well potential, which is strongly dependent on the hydrogen nuclear mass and the distribution of DADs. Thermal sampling of the DAD distribution gives rise to temperature dependent KIEs. Whereas, temperature independent KIEs reflect a narrow distribution of DADs peaked at short distances. The alternative model for the role of enzyme dynamics in hydride transfer reactions invokes protein promoting vibrations, which are non-statistical density fluctuations within the protein that modulate key properties of the reaction, such as the DAD. 15, <sup>40, 41</sup> The motions are identified on the basis of transition path sampling calculations of the enzyme-catalyzed reaction dynamics. These calculations identify compressive motions of the protein that serve to bring the donor and acceptor close together at the transition state, and the characteristic frequencies of the promoting vibrations are typically on the order of 100-150 cm<sup>-1</sup>. Although we analyze our results primarily in the context of the activated tunneling model, it is important to note that our experiments cannot, currently, differentiate between these two models. To the extent that there are equilibrium dynamics of the enzyme that are involved in narrowing the DAD distribution at the transition state, we expect that our spectroscopic studies will be sensitive to those motions.

This study compares the properties of the hydride-transfer step in WT FDH from *Candida boidinii* (CbFDH) with a series of active-site variants at position V123. V123 sits behind the nicotinamide ring of NAD<sup>+</sup> (Figure 1 B) and helps to optimize the donor-acceptor

distance (DAD) for efficient H-tunneling. Several previous studies of other enzymes have shown that similar mutations have significant effects on the hydride-transfer reaction that can be understood in terms of the effect of the mutation on the dynamics of DAD sampling. 42-44 Upon systematically reducing the size of the side chain via site-directed mutagenesis (V123A, V123G), we find that the KIEs on the hydride transfer catalyzed by FDH increase and that their temperature dependence also increases. This observation, along with the crystallographic (Figure 1 C) and molecular dynamics data, suggests that these mutations increase the average distance and broaden the overall distribution of distances between the donor and acceptor atoms. 44 Using 2D IR spectroscopy, we investigate the dynamics of ternary complexes of NAD<sup>+</sup> and azide bound to WT FDH and the V123 variants. These data reveal a correlation between the temperature dependence of KIEs and the amplitude of motions in the active site. We show that the mutations increase the amplitude of dynamics that likely reflect donor-acceptor fluctuations and are therefore relevant to the enzyme-catalyzed reaction. 37

## **Results and Discussion**

V123 is situated behind the C4 position of the nicotinamide in NAD+ and provides steric bulk to support a narrow DAD distribution peaked at a short distance (≤ 3.1Å) (Figure 1 B). Active site variants introduced at V123 perturb the DAD distribution at the TRS. From the crystal structure, this mutation appears to be on the line formed by the central nitrogen of the azide and the C4 of nicotinamide, opening space in the active site without disrupting the hydrogen bonds that hold azide in place. Steady-state kinetic parameters of the V123A and V123G CbFDH variants are summarized in the SI, and indicate that introduction of smaller active site residues at position 123 leads to lower activity. Previous experiments showed that WT FDH has a temperature-independent KIE,<sup>32</sup> suggesting that the active site is well organized for the hydride transfer.

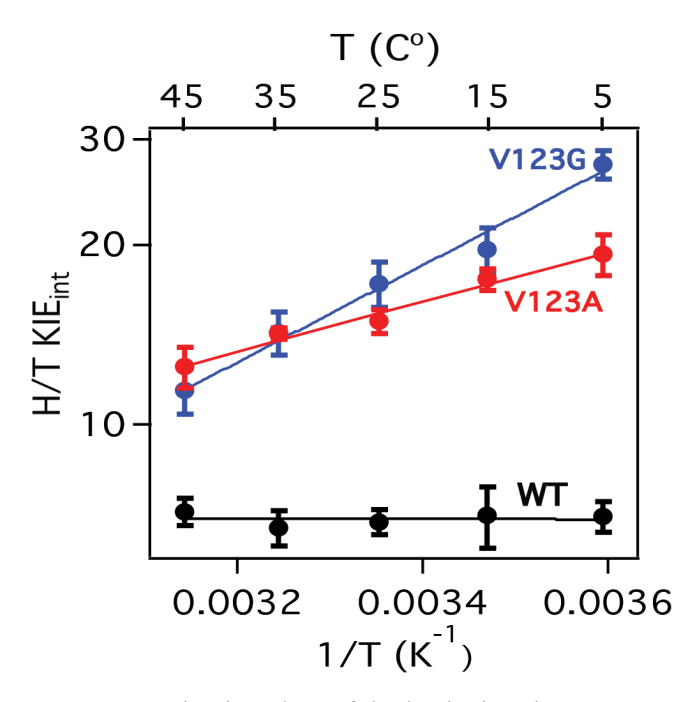


**Figure 2** Arrhenius plots of the intrinsic H/T KIEs (log scale) on the hydride transfer reaction catalyzed by wild-type (black), V123A (red) and V123G (blue) CbFDHs. Average KIEs are presented as points with their standard deviations. The lines are non-linear fits of all the data points to the Arrhenius equation.

Figure 2 summarizes the KIE results for the WT and variants of FDH in which we replace valine 123 with alanine or glycine and the values for observed D/T, H/T and intrinsic H/T KIEs are listed in the SI. The temperature dependence of the KIE increases as space is opened in the active site. We report the increase in the temperature dependence of the KIE as the change in activation energy ( $\Delta$  E<sub>H-T</sub>) for hydride transfer based on an Arrhenius equation analysis (Table 1.). The increasing

temperature dependence of the KIEs for the variant enzymes suggests that opening space in the active site perturbs the DAD distribution.

**Table 1.** Comparison of kinetic parameters from KIEs and measured donor acceptor distances (DAD) results between WT, V123A and V123G variants. The distance between the azide central nitrogen and the C4 carbon of NAD<sup>+</sup> as measured from X-ray crystal structures is analogous to the donor acceptor distance during the enzyme catalyzed hydride transfer. \*From Ref 29

	$A_{ m H}/A_{ m T}$	ΔE <sub>H-T</sub> (kcal/mol)	Average DAD (Å)	Deviation From WT(Å)
WT*	7 ± 2	$0.0 \pm 0.2$	$3.14 \pm 0.06$	-
V123A	$0.8 \pm 0.2$	$1.8 \pm 0.2$	$3.32\pm0.06$	$0.18\pm0.08$
V123G	$0.03\pm0.02$	$3.7 \pm 0.4$	$3.34 \pm 0.01$	$0.20\pm0.06$

We have previously observed an increase in temperature dependence in other systems, such as in dihydrofolate reductase, when the residue behind the nicotinamide was replaced with smaller residues.<sup>22</sup> Semiclassical transition state theory of over-the-barrier hydride transfer is

inconsistent with a temperature independent KIE for a temperature dependent rate constant and activated tunneling models for hydride transfer are required for interpreting the temperature dependence of the KIEs. 1, 7, 8 In these models, the reaction is assumed to proceed through quantum mechanical transfer for all of the isotopes, and, for short enough average DADs, the KIE can be smaller than the semi-classical maximum values predicted based on zero-point effects in an over-the-barrier reaction. Most importantly, the activated tunneling models indicate that the temperature dependence (or lack thereof) reflects donor-acceptor fluctuations about the average DAD, i.e. negligibly small amplitude conformational sampling of a narrow DAD distribution at short distances leads to the temperature independent KIE commonly observed in WT enzymes that perform hydride transfer efficiently. The increased temperature dependence observed with the mutations has thus been ascribed to a more flexible active site at the TRS compared to the WT enzyme. Upon mutation to less sterically bulky active-site residues, the average DAD will increase, and the DAD distribution will broaden. Thermal sampling of that distribution then becomes necessary to allow the reactants to approach distances where the hydride donor and acceptor are short enough to allow for efficient transfer of the hydrogen nucleus.

X-ray crystallography gives insights into the structural impacts caused by mutation at the V123 site, and also provides starting structures for molecular dynamics simulations. Data from these experiments allow us to examine the average structures of the complexes of azide bound with NAD<sup>+</sup> in the V123A (PDB 6D4B) and V123G (PDB 6D4C) variants and compare them to the published WT structure.<sup>32</sup> The crystal structures for the variants that we report are each at 1.45 Å resolution, which is comparable to the 1.50 Å resolution for the WT structure. The average DAD increases in going from WT to V123A or V123 G (Table 1.) These results

highlight importance of V123 in positioning the C4 of nicotinamide near the formate anion to accept a hydride during the enzyme-catalyzed reaction (Figure 1 C). The DAD difference between the variants and the WT is consistent with the inflation of the KIE for these variants. What the crystallography cannot report, however, is the distribution of DADs that is responsible for the temperature dependence of the KIEs.

2D IR spectroscopy reveals the equilibrium dynamics of the local environment around the azide anion, directly reporting the timescales of the structural fluctuations of the active site. 2D IR uses a series of short laser pulses to first excite and then probe the antisymmetric stretching frequency of the azide anion. At short time delays between excitation and detection, the local environment around the azide molecule remains unchanged. Thus, the frequency of the azide when it is probed correlates strongly with that at which it was originally excited, resulting in a peak elongated along the diagonal of the 2D IR spectrum. At increased waiting times, however, thermally-activated motions of the active site modulate the instantaneous frequency of the azide vibration during the time between excitation and detection, leading to a loss in correlation and rounding of the 2D IR lineshape. The timescales on which the lineshape changes report the azide frequency-frequency correlation function (FFCF) and reveal the timescales of those ensemble average dynamics of the active site that perturb the azide transition frequency. We use the centerline slope (CLS) analysis method<sup>45,46</sup> to analyze the 2D IR lineshapes. The CLS decay is directly proportional to the decay of the FFCF for the oscillator probed in a 2D IR experiment.

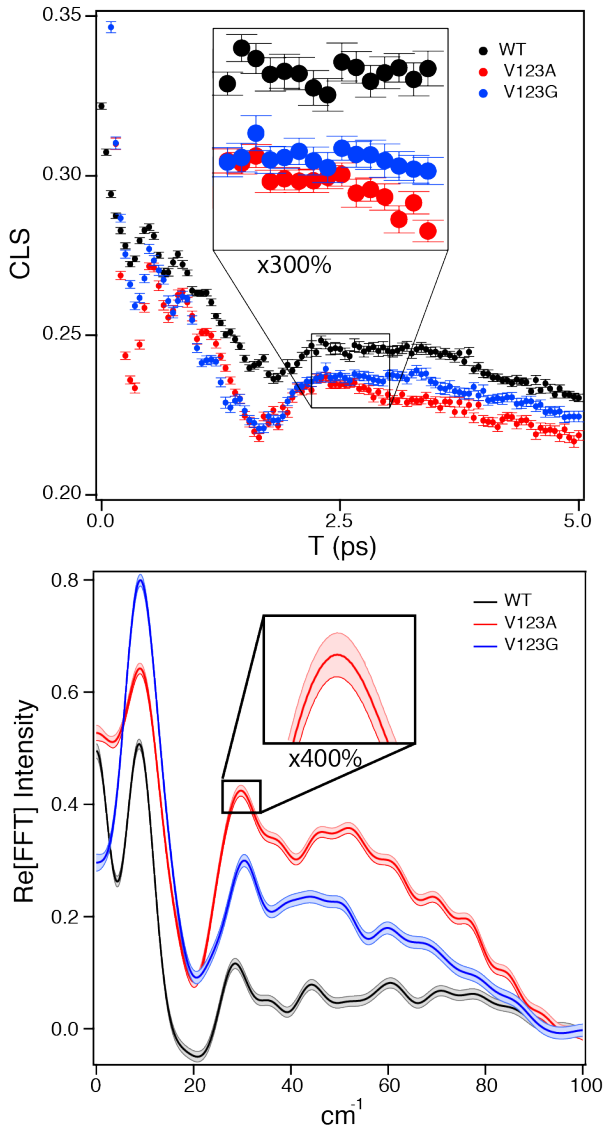


Figure 3 (upper panel) Center Line Slope (CLS) decay from the CLS analysis of the 2D IR spectra of azide in ternary complexes of NAD<sup>+</sup> with the WT (black), V123A (red) and V123G (blue) enzymes. Error bars (inset is 300% magnification) reflect the standard error of the mean for 80-100 replicate measurements at each waiting time. (lower panel) The real part of the Fast Fourier Transform (FFT) of the CLS decay after subtracting off the long timescale component of the decay that does not oscillate. Confidence bands on the FFTs (inset is 400% magnification) represent propagation of the standard error of means from the CLS values. Note the prominent feature at ~9 cm<sup>-1</sup> in each spectrum whose intensity increases systematically in the variants.

Figure 3 shows the time evolution of the CLS (upper panel) for azide bound to ternary complexes of CbFDH WT and variants with NAD+. For each waiting time, we collect 80-100 replicate 2D IR spectra and analyze the CLS value for each. The data points on the plot represent the mean of those values with error bars that correspond to the standard error of the mean (inset shows 300% magnification for clarity). As demonstrated previously,<sup>37</sup> the FFCF of the azide anion in this complex shows underdamped oscillations on the picosecond timescale. Like the WT enzyme, the V123A and V123G variants also exhibit underdamped oscillations on the ps timescale. The CLS decays do not evolve all of the way to zero on the 5.0 ps time scale, indicating that not all of the dynamics influencing the azide lineshape are sampled within this window. We have, however, also measured these decays out to 20 ps (Figure S4) to better fit the long timescale decay. As discussed in more detail in the SI, the high protein concentrations required for these

experiments make the samples susceptible to aggregation, which can have a significant effect on the observed CLS decay as Figure S3 illustrates. We have taken great care to ensure that our samples are free of the effects of aggregation and show now dependence on the protein concentration or the sample incubation time.

The lower panel of Figure 3 shows the Fast Fourier transforms (FFT) of the CLS decays after subtracting off the long time scale contribution. For each FFT, we show the uncertainties as a confidence band that results from propagating the standard error of the means accounting for the FFT (see inset for 400% magnification). The FFT can be thought of as a frequency spectrum of the protein motions as experienced by the azide reflecting the oscillatory frequencies that appear in the CLS decay. These low-frequency spectra are dominated by a peak centered at 9 cm<sup>-1</sup>, the amplitude of which increases on going from the WT to each of the variants. There are also distinct peaks at higher frequencies for both the WT and variant enzymes. Notably, the amplitudes of these higher frequencies are also larger in the variants, though they do not follow a consistent trend. In part, the amplitudes of these higher frequency motions are lower in V123G compared to V123A because the dephasing of the oscillations is more rapid as is evidenced by the broadening of the higher frequency bands in the FFT spectrum. Although these higher frequency modes are an interesting aspect of the data, we will focus our discussion on the trend observed in the 9 cm<sup>-1</sup> oscillation.

Previous examination of the oscillatory dynamics in the WT enzyme suggested that motions of the nicotinamide ring are likely responsible for the oscillating behavior in the FFCF of azide bound to FDH.<sup>37</sup> Because these mutations open up space behind the nicotinamide ring, any effect that mutations have on the fluctuation of the ring with respect to the azide are likely to perturb the oscillatory motions observed in the CLS decay. Thus, there is a strong expectation

that the mutations we have made should affect the amplitudes and/or frequencies of the oscillatory dynamics that we observe.

As already noted, the amplitude of the 9 cm<sup>-1</sup> mode increases systematically from the WT to V123A to V123G, consistent with the idea that there is more space in the active site allowing for a larger amplitude of this oscillatory motion.

Figure 4 shows that the amplitude of the low-frequency oscillatory component from the FFT of the CLS decay increases

linearly in proportion to  $\Delta E_{H-T}$ . If, as we

hypothesize, this oscillation reflects donor-

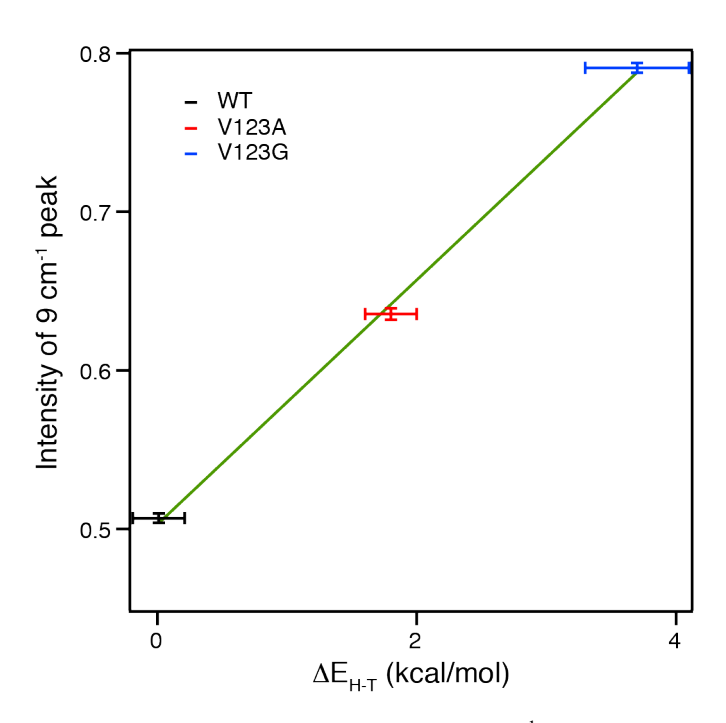


**Figure 4** Plot of the amplitude of the 9 cm<sup>-1</sup> peak in the FFT of the CLS decay from the 2D IR measurements versus the temperature dependence of the intrinsic KIE reported as the difference in activation energies between H and T isotopes in the hydride transfer reaction. The error bars on each measurement represent the 95% confidence intervals for the experimentally measured quantities. The green line is a linear fit to these data with a slope of 0.08±0.04 and an intercept of 0.50±0.08.

acceptor motions, it is easy to understand that the increase in space in the variants leads to an increase in the amplitude of the oscillatory motions that correlates with the increased DAD sampling reflected in the temperature dependence of the intrinsic KIE. This correlation consists of only three points because there are only two options among the set of natural amino acids for mutating V123 to a smaller hydrophobic residue, Ala and Gly. Other mutant variations are possible such as Ser, Cys, or Thr, for example, but we have avoided these variants out of concern that these residues could result in more substantial structural perturbations if the protic side-chain pursues a hydrogen bonding partner elsewhere in the active site. Nevertheless, having additional structural variants would be useful in future studies.

Although the correlation is easy to understand in a qualitative sense, it is much more difficult to quantitatively predict how the amplitude of the low-frequency motions of the active site should correlate with the width of the DAD. That this relationship should be approximately linear makes intuitive sense as both the width of the DAD and the amplitude of the oscillations reflect the amount of space available for the substrates to move before they encounter steric repulsions from the hydrophobic groups that pack the active site. Nevertheless, this intuitive picture is certainly oversimplified as reductions in the steric packing could also affect the long-range structure so as to prevent empty spaces within the protein. Thus, for very small changes in the size of the hydrophobic residues, as we have in this case, the expectation of a nearly linear correlation is probably correct and certainly consistent with our observations. Larger perturbations, however, could easily lead to significant nonlinear effects as a result of larger structural changes throughout the protein.

To better interpret our experimental results, we turn to molecular dynamic simulations of FDH ternary complexes. We first explore simulated trajectories of the azide-bound ternary complexes to see if the same oscillatory features we observe in the FFCF measured in the 2D IR experiments are also present in the simulation. We then look at free energy calculations of the hydride transfer reaction between formate and NADH to examine the distribution of structures at the ground state and the transition state. An in-depth description of the details of these simulations is available in the SI.

Figure 5 shows the force correlation functions (FCF) for the force projected onto the azide antisymmetric stretching mode from molecular dynamics trajectories for the azide-FDH-NAD+ ternary complexes in each of the enzymes. While there are quantitative differences in the

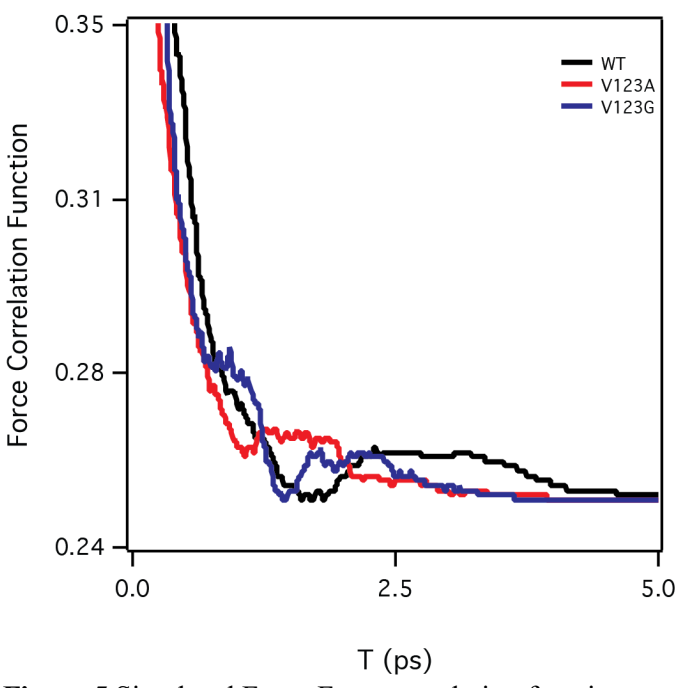


**Figure 5** Simulated Force-Force correlation functions for the force on the antisymmetric stretching coordinate of the azide anion in ternary complexes of azide with NAD<sup>+</sup> in the WT (black), V123A (red), and V123G (blue) enzymes.

amplitudes and frequencies of the oscillatory components between the simulation and the experiments, the FCFs agree qualitatively with the CLS decays from the 2D IR measurements. Fourier analysis of the FCFs show that the frequencies of the oscillations occur at approximately 10 and 20 cm<sup>-1</sup> and that the relative amplitude of the 10 cm<sup>-1</sup> oscillation increases on going from the WT to the V123A variant (see SI, Figure S5). The FCF for the V123G variant

shows more significant changes that do not agree with the experimental results from the 2D IR spectra.

In addition to the FCF, we also calculate the DAD distribution from the simulations as the histogram of distances between the central nitrogen of the azide and the C4 carbon of the nicotinamide ring (Figure 6). These distributions show a clear trend of increases both in the average DAD and in the width of the DAD distribution on

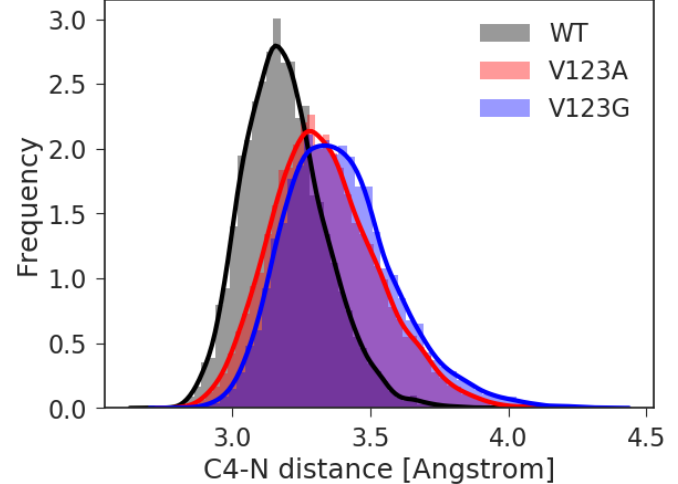


**Figure 6** Distribution of DADs calculated from simulations of ternary complexes of azide-NAD<sup>+</sup>-FDH for WT (black) and both V123A (red) and V123G (blue) variants.

going from the WT to the V123A to the V123G variants, consistent with our crystallographic measurements of the DAD in these complexes, though the size of the effect going from WT to V123A is much larger than the difference between V123A and V123G variants. The subtlety of the differences between the two mutant variants is consistent with the DAD distances reported in Table 1 from the crystal structures. These results are also consistent with what we would expect based on the KIE measurements. In the WT enzyme, the DAD is short enough that the H transfer probabilities for the isotopes are not very different as is evident from the relatively modest value of the KIE for the WT enzyme. The mutant variants exhibit both inflated and temperature dependent KIEs, but the differences in the KIE values and their temperature decencies for the two mutant variants are more modest relative to the difference between the WT and either mutant variant, which is consistent with the observed differences in the DADs in both the computational modeling and the crystallographic measurements. The qualitative agreement of the oscillatory contributions to the correlation functions between experiment and simulation and the trends in the DAD distribution support the conclusion that the observed behavior of azide in the 2D IR experiments are the result of oscillatory equilibrium motions in the active site whose amplitudes increase as we make mutations that increase the space available in the active site.

Table S5 gives the phenomenological free energy barriers,  $\Delta G^{\ddagger}$ , that we calculate from the experimentally observed  $k_{\text{cat}}$  values (Table S1) via Eyring's equation along with those determined from the classical and quantum mechanical potentials of mean force from QM/MM calculations of the hydride transfer reaction rate. Although chemistry is not fully rate limiting in FDH as is clear from the nonzero values of the commitment to catalysis that are evident based on the observed and intrinsic KIE values, the turnover rates reflect an upper bound on the chemistry and are sensitive to changes in the chemical step as the chemistry is partially rate limiting.<sup>32</sup> The

experimental  $\Delta G^{\ddagger}$  values for WT, V123A, and V123G are 16.4, 18.8, and 19.6 kcal/mol, respectively. The corresponding simulated multiscale free energy barriers for WT, V123A, and V123G reproduce the experimental trends reasonably well with  $\Delta G^{\ddagger}$  values of 13.5, 16.1, and 19.2 kcal/mol, respectively. DAD distributions can also be extracted from the QM/MM simulations in both the reactant state (RS) and the transition state (TS) using the distance between the C4 position of the nicotinamide ring and the central carbon of the substrate. Once again, we observe an increasing trend in average DAD and a broader distribution of DADs when mutating from WT to V123A to V123G (see SI, Figure S7), in agreement with measurements made from the crystal structures and in line with our interpretation from the KIE data. As would be expected, the effect of mutations on the DAD is much larger for the RS complexes than for the TS. Nevertheless, even the narrow distribution of DADs for the TS shows a slight increase in average distance for the variants. These results corroborate our interpretation of the temperature dependence of the KIEs in terms of the thermal sampling of the DAD distribution.

The simulations together with the experimental data provide compelling molecular insights into the equilibrium dynamics at the active site of FDH. Mutations of V123 increase the average DAD in both the reactive and azide-inhibited ternary complexes. The oscillatory features observed for the azide in FDH from the 2D IR experiments reflect relative motion of the hydride donor and acceptor and V123 is responsible for correct positioning of the substrates in the active site for efficient hydride tunneling. As mentioned in our previous publication,<sup>37</sup> the timescale for the oscillation observed in FDH is peculiar since it occurs at such low frequency (~10 cm<sup>-1</sup>). This motion is at much lower energy than the kinetic energy available from thermal fluctuations of the bath molecules (~200 cm<sup>-1</sup>), and would be expected to be overdamped in solution. It is also a much lower frequency than would be expected either for simple DAD fluctuations or for the

protein promoting vibrations that have been identified for other proteins, which are typically 100-150 cm<sup>-1</sup> motions. The basis for the observed underdamped behavior is unclear. One possibility is that the active site insulates the substrates from the thermal noise of the surrounding enzyme and solvent on the femtosecond to picosecond time scale. As the active site space opens as a result of mutations, the DAD distribution peaks at longer distance and broadens; the amplitude of the oscillatory dynamics increases, and thermally activated sampling of the DAD gives rise to temperature dependent KIEs. Another possibility is that the low frequency oscillation that we observe may be part of a more complicated and highly anharmonic mode of the protein, and we are only sensitive to the low frequency projection of this motion onto the azide anion. A better understanding of this motion is probably available from a careful analysis of the molecular dynamics simulations and will be the focus of future studies.

### **Conclusions**

This study shows the first correlation between equilibrium active site motions at the fs-ps timescale and the temperature dependence of KIEs on C-H-C bond activation in enzyme-catalyzed reactions. V123 acts to hold the H-acceptor (C4 position of the nicotinamide ring of the NAD<sup>+</sup>) close to the H-donor (formate) in FDH. In this way, WT FDH is able to pack the space in the active site as efficiently as possible to minimize the distance for hydrogen tunneling. Upon mutagenesis, increased temperature dependence of the KIE correlates with the increasing amplitude of oscillations in the frequency fluctuations of the azide anion bound to FDH, indicating that 1) V123 is at least partly responsible for the narrow DAD distribution identified for the WT FDH by the temperature independent KIEs; 2) the oscillations observed in the frequency fluctuations of the azide are sensitive to donor-acceptor dynamics, and 3) the less compact structure of the active site in variant FDHs increases the DAD, which impacts donor-

acceptor motions at the fs-ps timescale in ways that increase activation free energy for hydride transfer. By means of other structural or environmental variations (isotope labeling, further mutation, temperature dependences) we plan to continue to use FDH as a model system to understand the molecular origin of the oscillatory dynamics in more detail and how structural fluctuations at the fs-ps timescale influence enzyme-catalyzed hydride transfer.

### **METHODS**

Materials –The primers for active site variants were prepared by Integrated DNA Technologies. QuikChange II Site-Directed Mutagenesis Kits were purchased from Agilent Technologies. *E. coli* BL21 (DE3) pLysS cells were from Novagen. Blue sepharose 6 fast flow and Superdex 200 resin were from GE Healthcare Life Sciences. Bradford dye reagent, SDS gels and the protein standards were from Bio-Rad. [Ad-14C]-NAD+ was from PerkinElmer. [3H]-formic acid was from Moravek Biochemicals. All other materials were purchased from Sigma-Aldrich unless otherwise specified.

Site directed mutagenesis was performed on the gene for WT FDH, using standard procedures, and the primer design is listed in the SI. Plasmids were transformed into BL21 (DE3) pLysS cells and grown in 6 L Luria-Bertani medium with 100 mg/L ampicillin at 37°C and 250 rpm. Expression and purification of WT and variant FDHs were carried out using the procedure in Ref. 29.

**Steady-state kinetics** – The  $K_{\text{M/NAD}^+}$  and  $k_{\text{cat}}$  were determined through initial velocity studies by varying the NAD+ concentration from 0.02 to 12 mM at a formate concentration of 200 mM. The production of NADH was monitored by following UV absorption at 340 nm in 100 mM phosphate buffer at pH 7.5 and 25°C. The reaction was initiated by adding 0.2  $\mu$ M

CbFDH (final concentration). Similarly,  $K_{\text{M/formate}}$  was measured under the same buffer and enzyme concentration by varying the formate concentration from 1 to 215 mM at a NAD+ concentration of 10 mM. Data were fit to the Michaelis–Menten equation to obtain the kinetic parameters  $k_{\text{cat}}$  and  $K_{\text{M}}$  for both substrates.

Kinetic isotope effect measurements – We measure both H/T and D/T competitive KIEs to determine the intrinsic KIEs for native and mutant variants of CbFDH at 5, 15, 25, 35 and 45 °C using the procedure described previously.<sup>29</sup> Briefly, for the H/T experiment, in 1 ml final volume of 100 mM phosphate buffer (pH 7.5), trace amounts of [Ad-14C]-NAD+(660,000 dpm) and [3H]-formic acid (3,300,000 dpm) mix with 50 mM NAD+ and 40 mM formic acid. Similarly for D/T experiment we use 40mM 99.8% deuterated formic acid. During the reaction, the hydride or deuteride transfers from formic acid to [Ad-<sup>14</sup>C]- NAD+ to form [Ad-<sup>14</sup>C]-NADH/D. Similarly, [3H]-NADH forms as a result of transfer from [3H]-formic acid. Therefore, [Ad-14C]-NADH/D track the protium or deuterium transferred, and [3H]-NADH tracks the tritium transferred. The reaction initiates by addition of CbFDH, and removing 100  $\mu$ l aliquots at different timepoints yields various fractional conversions that are quenched by adding 20 µl of 50 mM azide. All samples are immediately frozen on dry ice and then kept at -80 °C until analyzed on the HPLC. The HPLC separation is followed by liquid scintillation counter (LSC) analysis to determine the depletion of <sup>3</sup>H relative to <sup>14</sup>C in the product at different fractional conversions. The observed KIEs are calculated using eq. (1)

$$KIE = \frac{\ln(1 \square f)}{\ln \left| \prod f \left( R_{t} / R_{\square} \right) \right|}$$
(1)

where f is the fractional conversion based on  $^{14}\text{C-NAD}^+$  and  $R_t$  and  $R_{\infty}$  are the isotope ratios between  $^3\text{H}$  and  $^{14}\text{C}$  at time t and infinity, respectively. We measure 5 observed H/T and D/T KIEs for each temperature.

$$f = \frac{[^{14}\text{C}]\text{NADH}}{(100\text{-}\%\text{excess})([^{14}\text{C}]\text{NADH} + [^{14}\text{C}]\text{NAD}^{+})} (2)$$

$$R = \frac{{}^{3}\mathrm{H}_{\mathrm{NADH}}}{{}^{14}\mathrm{C}_{\mathrm{NADH}}}$$
 (3)

We calculate intrinsic KIEs from the observed values using a numerical solution of the modified Northrop equation: 47,48

$$\frac{{}^{T}(V/K)_{Hobs}^{-1} - 1}{{}^{T}(V/K)_{Dobs}^{-1} - 1} = \frac{(k_{H}/k_{T})^{-1} - 1}{(k_{H}/k_{T})^{-1/3.34} - 1}$$
(4)

where  $k_{\rm H}/k_{\rm T}$  is the intrinsic H/T KIE and  $^{\rm T}(V/K)_{\rm H,obs}$  and  $^{\rm T}(V/K)_{\rm D,obs}$  are the observed H/T and D/T KIE values for the second-order rate constant  $k_{\rm cat}/K_{\rm M}$ , respectively. As there were 5 H/T and D/T observed KIEs for each temperature, 25 pairs are used to calculate the intrinsic KIE value for each temperature.

X-Ray Crystallography- V123A and V123G crystals were obtained using previously established procedures<sup>32</sup> using the ALS beamline 4.2.2. Crystallization conditions were set to generate ternary complexes with NAD<sup>+</sup> and azide. The two V123 variants crystallized in the same crystal form as WT FDH under the following conditions: 0.1 M HEPES, 25% PEG 3350, pH 7.5. Detailed X-ray data are summarized in the supporting information. Both protein crystals were grown under 50X excess (50mM) of NAD+ and azide relative to the ~1.0 mM enzyme concentration to ensure that all of the enzyme active sites were prebound upon crystallization. Error associated with each DAD listed in Table 1 was known as the coordinate error and was generated from the B-factors after the latest phenix-refinement.

**2D IR spectroscopy-** The apparatus and sample preparation for 2D IR measurements has been described previously and is detailed in the SI.<sup>37, 49</sup> To extract the dynamics from 2D IR spectra we determine the CLS values at each waiting time. The reported data are the mean of 80-100 replicates at each waiting time with error bars given by the standard error of means.

**Molecular Dynamics Simulations**- Detailed information is available in the Supporting Information.

### SUPPORTING INFORMATION AVAILABLE

Description of site-directed mutations; steady-state kinetic parameters for all variants; Isothermal titration calorimetry data for the mutant variants; X-Ray data collection and refinement statistics; more details of the 2D IR apparatus, experimental conditions, and data analysis; detailed information about the MD simulations and the QM/MM simulations

# **ACKNOWLEDGMENTS**

This work was supported by grants from the NIH GM079368 to CMC and AK and NSF CHE 1707598 to CMC and the United States-Israel Binational Science Foundation (Grant # 2012340) to AK and DTM. FH acknowledges support from the Herchel Smith Graduate Fellowship. Azide force correlation calculations were completed on the Odyssey cluster supported by the FAS Division of Science, Research Computing Group at Harvard University. This work was funded by the Center for Excitonics, an Energy Frontier Research Center funded by the U.S. Department of Energy, Office of Science and Office of Basic Energy Sciences, under Award Number DE-SC0001088. (AAG and FH). We thank Dr. Nikolaos Labrou from Agricultural University of Athens for providing us with the recombinant CbFDH plasmid.

# References

- 1. Klinman, J. P.; Kohen, A., Hydrogen Tunneling Links Protein Dynamics to Enzyme Catalysis. *Annual Review of Biochemistry, Vol 82* **2013**, *82*, 471-496.
- 2. Glowacki, D. R.; Harvey, J. N.; Mulholland, A. J., Taking Ockham's razor to enzyme dynamics and catalysis. *Nature Chemistry* **2012**, *4*, 169.
- 3. Hay, S.; Scrutton, N. S., Good vibrations in enzyme-catalysed reactions. *Nature Chemistry* **2012**, *4* (3), 161-168.
- 4. Kamerlin, S. C. L.; Warshel, A., At the dawn of the 21st century: Is dynamics the missing link for understanding enzyme catalysis? *Proteins: Structure, Function, and Bioinformatics* **2010,** 78 (6), 1339-1375.
- 5. Nagel, Z. D.; Klinman, J. P., A 21(st) century revisionist's view at a turning point in enzymology. *Nature Chemical Biology* **2009**, *5* (8), 543-550.
- 6. Palmer, A. G., Enzyme Dynamics from NMR Spectroscopy. *Accounts of Chemical Research* **2015**, *48* (2), 457-465.
- 7. Kohen, A., Role of Dynamics in Enzyme Catalysis: Substantial versus Semantic Controversies. *Accounts of Chemical Research* **2015**, *48* (2), 466-473.
- 8. Klinman, J. P., Dynamically Achieved Active Site Precision in Enzyme Catalysis. *Accounts of Chemical Research* **2015**, *48* (2), 449-456.
- 9. McGeagh, J. D.; Ranaghan, K. E.; Mulholland, A. J., Protein dynamics and enzyme catalysis: Insights from simulations. *BBA Proteins and Proteomics* **2011**, *1814* (8), 1077-1092.
- 10. Truhlar, D. G., Transition state theory for enzyme kinetics. *Arch Biochem Biophys* **2015**, *582*, 10-17.
- 11. Antoniou, D.; Schwartz, S. D., Protein Dynamics and Enzymatic Chemical Barrier Passage. *Journal of Physical Chemistry B* **2011**, *115* (51), 15147-15158.
- 12. Schwans, J. P.; Hanoian, P.; Lengerich, B. J.; Sunden, F.; Gonzalez, A.; Tsai, Y.; Hammes-Schiffer, S.; Herschlag, D., Experimental and Computational Mutagenesis To Investigate the Positioning of a General Base within an Enzyme Active Site. *Biochemistry* **2014**, *53* (15), 2541-2555.
- 13. Cheatum, C. M.; Kohen, A., Relationship of Femtosecond–Picosecond Dynamics to Enzyme-Catalyzed H-Transfer. In *Dynamics in Enzyme Catalysis*, Hammes-Schiffer, S.; Klinman, J., Eds. Springer Berlin Heidelberg: 2013; Vol. 337, pp 1-39.
- 14. Of polemics and progress. *Nat Chem* **2012**, *4* (3), 141-141.
- 15. Schramm, V. L.; Schwartz, S. D., Promoting Vibrations and the Function of Enzymes. Emerging Theoretical and Experimental Convergence. *Biochemistry* **2018**, *57* (24), 3299-3308.
- 16. Varga, M. J.; Dzierlenga, M. W.; Schwartz, S. D., Structurally Linked Dynamics in Lactate Dehydrogenases of Evolutionarily Distinct Species. *Biochemistry* **2017**, *56* (19), 2488-2496.
- 17. Pineda, J.; Schwartz, S. D., Protein dynamics and catalysis: the problems of transition state theory and the subtlety of dynamic control. *Philosophical Transactions of the Royal Society B-Biological Sciences* **2006**, *361* (1472), 1433-1438.
- 18. Silva, R. G.; Murkin, A. S.; Schramm, V. L., Femtosecond dynamics coupled to chemical barrier crossing in a Born-Oppenheimer enzyme. *Proceedings of the National Academy of Sciences of the United States of America* **2011**, *108* (46), 18661-18665.
- 19. Benkovic, S. J.; Hammes-Schiffer, S., A Perspective on Enzyme Catalysis. *Science* **2003**, *301* (5637), 1196-1202.

- 20. Wang, Z.; Abeysinghe, T.; Finer-Moore, J. S.; Stroud, R. M.; Kohen, A., A Remote Mutation Affects the Hydride Transfer by Disrupting Concerted Protein Motions in Thymidylate Synthase. *J Am Chem Soc* **2012**, *134* (42), 17722-17730.
- 21. Singh, P.; Sen, A.; Francis, K.; Kohen, A., Extension and Limits of the Network of Coupled Motions Correlated to Hydride Transfer in Dihydrofolate Reductase. *Journal of the American Chemical Society* **2014**, *136* (6), 2575-2582.
- 22. Francis, K.; Stojkovic, V.; Kohen, A., Preservation of Protein Dynamics in Dihydrofolate Reductase Evolution. *Journal of Biological Chemistry* **2013**, *288* (50), 35961-35968.
- 23. Pudney, C. R.; Guerriero, A.; Baxter, N. J.; Johannissen, L. O.; Waltho, J. P.; Hay, S.; Scrutton, N. S., Fast Protein Motions Are Coupled to Enzyme H-Transfer Reactions. *Journal of the American Chemical Society* **2013**, *135* (7), 2512-2517.
- 24. Nagel, Z. D.; Cun, S.; Klinman, J. P., Identification of a long-range protein network that modulates active site dynamics in extremophilic alcohol dehydrogenases. *J Biol Chem* **2013**, *288* (20), 14087-97.
- 25. Liang, Z. X.; Lee, T.; Resing, K. A.; Ahn, N. G.; Klinman, J. P., Thermal-activated protein mobility and its correlation with catalysis in thermophilic alcohol dehydrogenase. *Proceedings of the National Academy of Sciences of the United States of America* **2004**, *101* (26), 9556-9561.
- 26. Núñez, S.; Wing, C.; Antoniou, D.; Schramm, V. L.; Schwartz, S. D., Insight into Catalytically Relevant Correlated Motions in Human Purine Nucleoside Phosphorylase. *J Phys Chem A* **2006**, *110* (2), 463-472.
- 27. Unden, G.; Kroger, A., Reconstitution of a functional electron-transfer chain from purified formate dehydrogenase and fumarate reductase complexes. *Methods Enzymol* **1986**, *126*, 387-99.
- 28. Blanchard, J. S.; Cleland, W. W., Kinetic and Chemical Mechanisms of Yeast Formate Dehydrogenase. *Biochemistry* **1980**, *19* (15), 3543-3550.
- 29. Bandaria, J. N.; Cheatum, C. M.; Kohen, A., Examination of Enzymatic H-Tunneling through Kinetics and Dynamics. *Journal of the American Chemical Society* **2009**, *131* (29), 10151-10155.
- 30. Torres, R.; Schøtt, B.; Bruice, T. C., Molecular dynamics simulations of ground and transition states for the hydride transfer from formate to NAD<sup>+</sup> in the active site of formate dehydrogenase. *J. Am. Chem.Soc.* **1999**, *121*, 8164-8173.
- 31. Popov, V. O.; Lamzin, V. S., Nad(+)-Dependent Formate Dehydrogenase. *Biochemical Journal* **1994**, *301*, 625-643.
- 32. Guo, Q.; Gakhar, L.; Wickersham, K.; Francis, K.; Vardi-Kilshtain, A.; Major, D. T.; Cheatum, C. M.; Kohen, A., Structural and Kinetic Studies of Formate Dehydrogenase from Candida boidinii. *Biochemistry* **2016**, *55* (19), 2760-2771.
- 33. Hill, S. E.; Bandaria, J.; Fox, M.; Vanderaugh, E.; Kohen, A.; Cheatum, C. M., Exploring the Molecular Origins of Protein Dynamics in the Active Site of Human Carbonic Anhydrase II. *Journal of Physical Chemistry B* **2009**, *113* (33), 11505-11510.
- 34. Thielges, M. C.; Axup, J. Y.; Wong, D.; Lee, H. S.; Chung, J. K.; Schultz, P. G.; Fayer, M. D., Two-Dimensional IR Spectroscopy of Protein Dynamics Using Two Vibrational Labels: A Site-Specific Genetically Encoded Unnatural Amino Acid and an Active Site Ligand. *Journal of Physical Chemistry B* **2011**, *115* (38), 11294-11304.

- 35. Gundogdu, K.; Bandaria, J.; Nydegger, M.; Rock, W.; Cheatum, C. M., Relaxation and anharmonic couplings of the O-H stretching vibration of asymmetric strongly hydrogen-bonded complexes. *Journal of Chemical Physics* **2007**, *127* (4), 044501.
- 36. Bandaria, J. N.; Dutta, S.; Nydegger, M. W.; Rock, W.; Kohen, A.; Cheatum, C. M., Characterizing the dynamics of functionally relevant complexes of formate dehydrogenase. *Proceedings of the National Academy of Sciences of the United States of America* **2010**, *107* (42), 17974-17979.
- 37. Pagano, P.; Guo, Q.; Kohen, A.; Cheatum, C. M., Oscillatory Enzyme Dynamics Revealed by Two-Dimensional Infrared Spectroscopy. *Journal of Physical Chemistry Letters* **2016**.
- 38. Meyer, M. P.; Tomchick, D. R.; Klinman, J. P., Enzyme structure and dynamics affect hydrogen tunneling: The impact of a remote side chain (1553) in soybean lipoxygenase-1. *Proceedings of the National Academy of Sciences of the United States of America* **2008**, *105* (4), 1146-1151.
- 39. Bahnson, B. J.; Colby, T. D.; Chin, J. K.; Goldstein, B. M.; Klinman, J. P., A link between protein structure and enzyme catalyzed hydrogen tunneling. *Proceedings of the National Academy of Sciences of the United States of America* **1997**, *94* (24), 12797-12802.
- 40. Schwartz, S. D., Protein Dynamics and the Enzymatic Reaction Coordinate. In *Dynamics in Enzyme Catalysis*, Klinman, J.; HammesSchiffer, S., Eds. Springer-Verlag Berlin: Berlin, 2013; Vol. 337, pp 189-208.
- 41. Schwartz, S. D.; Schramm, V. L., Enzymatic transition states and dynamic motion in barrier crossing. *Nature Chemical Biology* **2009**, *5* (8), 552-559.
- 42. Caratzoulas, S.; Mincer, J. S.; Schwartz, S. D., Identification of a protein-promoting vibration in the reaction catalyzed by horse liver alcohol dehydrogenase. *Journal of the American Chemical Society* **2002**, *124* (13), 3270-3276.
- 43. Nagel, Z. D.; Meadows, C. W.; Dong, M.; Bahnson, B. J.; Klinman, J. P., Active Site Hydrophobic Residues Impact Hydrogen Tunneling Differently in a Thermophilic Alcohol Dehydrogenase at Optimal versus Nonoptimal Temperatures. *Biochemistry* **2012**, *51* (20), 4147-4156.
- 44. Stojković, V.; Perissinotti, L. L.; Willmer, D.; Benkovic, S. J.; Kohen, A., Effects of the Donor–Acceptor Distance and Dynamics on Hydride Tunneling in the Dihydrofolate Reductase Catalyzed Reaction. *Journal of the American Chemical Society* **2012**, *134* (3), 1738-1745.
- 45. Kwak, K.; Rosenfeld, D. E.; Fayer, M. D., Taking apart the two-dimensional infrared vibrational echo spectra: More information and elimination of distortions. *Journal of Chemical Physics* **2008**, *128* (20), 204505.
- 46. Guo, Q.; Pagano, P.; Li, Y.-L.; Kohen, A.; Cheatum, C. M., Line shape analysis of two-dimensional infrared spectra. *Journal of Chemical Physics* **2015**, *142* (21).
- 47. Cook, P. F.; Cleland, W. W., *Enzyme Kinetics and Mechanism*. Taylor and Francis Group LLC: New York, NY, 2007.
- 48. Quirk, D. J.; Northrop, D. B., Effect of Pressure on Deuterium Isotope Effects of Formate Dehydrogenase. *Biochemistry* **2000**, *40* (3), 847-851.
- 49. Rock, W.; Li, Y. L.; Pagano, P.; Cheatum, C. M., 2D IR Spectroscopy using Four-Wave Mixing, Pulse Shaping, and IR Upconversion: A Quantitative Comparison. *Journal of Physical Chemistry A* **2013**, *117* (29), 6073-6083.

